

# Electrochemical tuning of band structure of single-walled carbon nanotubes probed by *in situ* resonance Raman scattering

Shankar Ghosh and A. K. Sood<sup>a)</sup>

Department of Physics, Indian Institute of Science, Bangalore-560 012, India

C. N. R. Rao

Jawaharlal Nehru Center for Advanced Scientific Research, Jakkur Campus, Jakkur P.O., Bangalore-560 064, India

*In situ* resonance Raman scattering of single-walled carbon nanotubes investigated under electrochemical biasing demonstrates that the intensity of the radial breathing mode varies significantly in a nonmonotonic manner as a function of the cathodic bias voltage, but does not change appreciably under anodic bias. The tangential mode is, however, not affected. These results can be quantitatively understood in terms of the changes in the energy gaps between the one-dimensional van Hove singularities in the electron density of states arising possibly due to the alterations in the overlap integral of  $\pi$  bonds between the  $p$  orbitals of the adjacent carbon atoms.

There is an overwhelming interest in single-wall carbon nanotubes (SWNT) originating from their unique geometrical, mechanical, electronic and chemical properties.<sup>1-3</sup> Carbon Nanotubes have also been shown to be excellent actuators<sup>4</sup> where the actuating action has been attributed not to the intercalation of ions, but due to the electrochemical double layer charging. This, in turn, is expected to change the electronic structure of the nanotubes. Our motivation is to quantify the effect of the electrochemical biasing of the nanotubes on the electronic band structure over and above the doping. This has been achieved by employing resonance Raman scattering (RRS) which probes both vibrational and electronic states. Raman spectra of SWNT shows two prominent bands: one near  $\sim 180\text{ cm}^{-1}$  associated with the radial breathing mode (RBM) and the other near  $1590\text{ cm}^{-1}$  attributed to the tangential modes (TM). The frequency of the radial mode depends inversely on the tube diameter and the van der Waals interaction between the tubes assembled in bundles. The resonant scattering process arises from the one-dimensional (1D) van Hove singularities in the electronic density of states with energy gaps which depend inversely on the tube diameter.<sup>5</sup> Thus, the diameter-selective RRS has been effectively used to determine the mean diameter, width of the diameter distribution and the van der Waals interaction between the nanotubes in a bundle.<sup>6,7</sup>

*In situ* micro-Raman scattering experiments were carried out using 50X long working distance objective in a back-scattering geometry. Raman spectra were excited using 514.5 nm ( $E_L=2.41\text{ eV}$ ) and 457.9 nm ( $E_L=2.71\text{ eV}$ ) radiations from an argon ion laser with power of  $\sim 1\text{ mW}$  on the sample. A DILOR-XY spectrometer equipped with liquid nitrogen cooled charge coupled device detector was used. SWNT bundles were prepared by electric arc method fol-

lowed by purification processes as explained in our earlier work.<sup>8</sup> The average diameter ( $d_0$ ) of the nanotubes was 1.5 nm. Single wall carbon nanotube bundles formed one electrode in an electrochemical cell and platinum was used as a counter electrode. The electrolyte used was 0.05 M LiClO<sub>4</sub>. The open circuit voltage of the cell was  $-0.6\text{ mV}$ . The nanotubes were in the form of a pellet (thickness  $\sim 100\text{ }\mu\text{m}$ ) whose ohmic contacts were electrically insulated from the electrolyte. The focusing of the SWNT electrode was constantly monitored under the microscope. Raman spectra were recorded as a function of the bias voltage ( $v$ ), both negative (cathodic) and positive (anodic). In order to avoid transient effects at every value of the bias voltage, the cell was allowed to stabilize to a constant current before Raman measurements were done.

Figure 1 shows the Raman bands due to RBM and TM (in the inset) at zero bias [curve (a)], and at a bias of  $-0.08\text{ V}$  [curve (b)] using  $E_L=2.41\text{ eV}$ . For the RBM, the solid lines represent the data and the dotted lines are the calculated line shapes (to be explained later). Figure 2 shows the integrated intensities of the Raman bands by filled circles ( $E_L=2.41\text{ eV}$ ) and filled stars ( $E_L=2.71\text{ eV}$ ). The intensities in Fig. 2 have been normalized with respect to the intensities under open circuit condition. Most interestingly, we see that on the application of the negative bias on the SWNT electrode with respect to the Pt counter electrode, the intensity of the RBM shows significant nonmonotonic changes, being very different for the two exciting laser energies. For low bias voltage (less than 0.05 V) the intensity increases when  $E_L=2.41\text{ eV}$ , in sharp contrast to the case when  $E_L=2.71\text{ eV}$ . These changes in intensity are reversible on removal of the bias. Furthermore, the TM intensity is not affected by cathodic as well as anodic bias. There is no shift in the frequency of RBM and TM with the applied bias. This can be understood on the basis that at such low bias voltages the charge transfer per carbon atom is very small. To esti-

<sup>a)</sup> Author to whom correspondence should be addressed; electronic mail: asood@physics.iisc.ernet.in

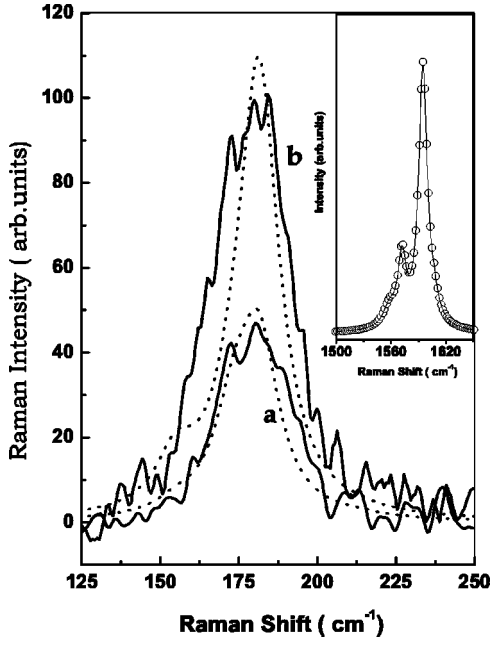


FIG. 1. Experimental Raman spectra (solid lines) of the RBM at zero bias (a) and  $-0.08$  V (b) for  $E_L = 2.41$  eV. The dotted lines show the calculated line shapes. Inset shows the observed Raman spectra in the TM regime at zero bias (open circles) and at  $-0.08$  V (solid line)

mate the doping we note that the effective capacitance of the nanotubes is  $\sim 20$  F/g m<sup>4</sup>. A potential difference of  $0.2$  V implies a capacitive charge of about  $1$  e/2000 carbon atoms. Since the frequency shift of the TM is about  $-140$  cm<sup>-1</sup> per electron doping of carbon atom and about  $460$  cm<sup>-1</sup> per hole doping,<sup>9</sup> such small doping will not produce observable shifts in the Raman spectra. However, a small frequency shift ( $\sim 4$  cm<sup>-1</sup>) in the TM at higher bias voltages due to electrolytic doping has been seen.<sup>10</sup>

We now discuss the nonmonotonic variation of the intensity of the RBM as a function of cathodic bias (cf. Fig. 1). This variation can be understood as due to the changes in the resonance Raman condition associated with the bias-dependent effects on the electronic structure of nanotubes. The electronic excitations in the nanotubes participating in

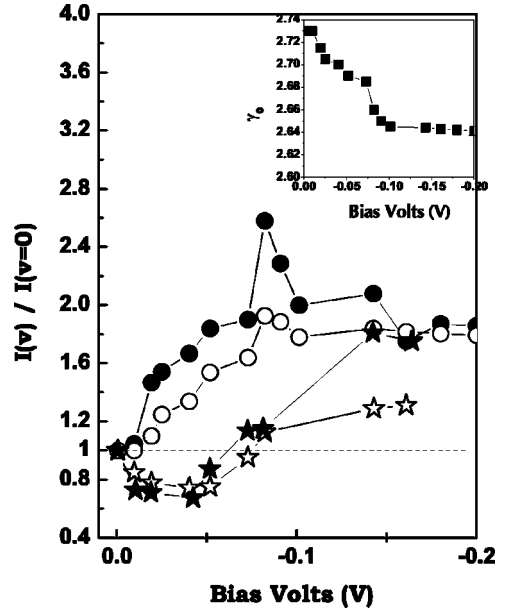


FIG. 2. Variation of the integrated intensities of the modes normalized with respect to the zero bias spectra for RBM (circles for  $E_L = 2.41$  eV, stars for  $E_L = 2.71$  eV). Solid symbols are experimental data. Open symbols correspond to the calculated intensities with  $\gamma(v)$  as the only adjustable parameter. The voltage dependence of  $\gamma(v)$  is same for both  $E_L$ 's. Inset shows variation of the overlap integral  $\gamma_0$ , with the applied bias voltage ( $v$ ).

Raman scattering are the transitions of electrons from the  $i$ th valence band singularity ( $v_i$ ) to the  $j$ th conduction band singularity ( $c_j$ ). However, symmetry reasons allow only  $v_i \rightarrow c_i$ . Within the tight binding approximation, the energy gap between  $v_i$  and  $c_i$  van Hove singularities is given by,<sup>5,11</sup>  $E_{ii} = 2i\gamma_0 a_{cc}/d + \delta E$ . Here,  $\gamma_0$  is the  $pp\pi$  overlap integral between the nearest-neighbor carbon atoms separated by the distance  $a_{cc}$  ( $= 0.142$  nm). For semiconducting tubes,  $i = 1, 2, 4, 5, \dots$  and for metallic tubes  $i = 3, 6, \dots$ . The second term arises due to van der Waals interaction between the nanotubes in a bundle and its magnitude is  $\sim 0.2$  eV.<sup>11</sup> Resonant enhancement occurs both for the incident (incoming resonance) as well as the scattered photons (outgoing resonance).

The Raman line shape can be written as<sup>6</sup>

$$I(\omega) = \sum_{\omega_{ph}} \left( A \sum_{i=1}^{15} \sum_d \frac{1}{d^2} \frac{p(d)}{((E_{ii} - E_L)^2 + \Gamma_e^2)((E_{ii} - (E_L - \hbar\omega_{ph}))^2 + \Gamma_e^2)} \right) \frac{\Gamma}{4(\omega - \omega_{ph})^2 + \Gamma^2}, \quad (1)$$

where  $\omega_{ph}$  is the phonon frequency,  $\Gamma$  (full width at half maximum) is the phonon damping constant. The term in the parenthesis is the Stokes Raman cross section from a collection of nanotubes with diameter distribution  $p(d)$ ,  $1/d^2$  is the contribution from the joint density of electronic states.  $\Gamma_e$  is the broadening parameter for the electronic bands. The distribution of diameters were taken to be a Gaussian centered at  $d_0$ :  $p(d) \sim e^{-(d-d_0)^2/2\sigma^2}$ , taking  $\sigma$  to be  $0.08$  nm. The parameter  $A$  contains all three matrix elements related to elec-

tron radiation and electron-phonon interaction Hamiltonians which are assumed to be constant.<sup>6</sup> The RBM frequencies have a diameter dependence given by<sup>7</sup>  $\omega_{ph} = 234/d + 12d$ , where  $\omega_{ph}$  is in units of cm<sup>-1</sup> and  $d$  in units of nm. The second term arises due to the van der Waals intertube interactions. The tangential modes have no dependence on  $d$ . The resonance width  $\Gamma_e = 0.05$  eV and  $\Gamma = 15$  cm<sup>-1</sup> were found to be appropriate to match the calculated and experimental spectra. For zero bias conditions, the value of  $\gamma_0$  obtained

from the best fit of the data ( $E_L=2.41$  eV) to Eqs. (1) was found to be 2.73 eV, which is well in accordance with the reported values.<sup>6,7,12</sup> The calculated line shape is shown in Fig. 2 by the solid line [curve (a)] which fits the experimental data well. The constant A, obtained by normalizing the observed  $1594\text{ cm}^{-1}$  TM peak intensity for zero bias condition with the calculated one, was kept constant subsequently for line shape analysis of the RBM at all bias voltages. Although the summation over the order of the electronic transitions was done for  $i=1-15$ , the main contribution to the Raman intensity comes from the  $i=4$  electronic transition ( $E_{44}\sim 2.3$  eV).

We argue that the cathodic bias voltage alters only the value of  $\gamma_0$  which in turn alters  $E_{ii}$ , thereby changing the Raman intensity [cf. Eq. (1)]. The skin depth of the incident radiation ( $E_L=2.41$  eV) in SWNT is about 200 nm,<sup>13</sup> and the contribution to the Raman signal comes, therefore, from the interface of the SWNT electrode with the electrolyte as well as from the underlying bulk sample. Since the effect of the space charge layer is mostly felt by surface of the SWNT electrode, we propose a two layer model as follows. The Raman intensity from the SWNT electrode is a sum of two contributions—one from the surface layer with  $\gamma_0=\gamma(v)$  and the other from the underlying unaffected bulk with  $\gamma_0=2.73$  eV. In order to avoid additional parameters, these two contributions were taken to be equal, i.e.,  $I(\omega, v) = \frac{1}{2}[I(\omega, \gamma(v)) + I(\omega, \gamma(v=0))]$ .

Experimental data for the finite cathodic bias were fitted using Eqs. (1), with only *one* adjustable parameter,  $\gamma(v)$ . The dotted line in curve (b) of Fig. 2 shows the calculated line shape with  $\gamma(v=-0.08\text{ V})=2.64$  eV. The agreement between experimental and calculated line shapes is reasonable. The voltage dependence of  $\gamma_0$  obtained from analyzing the Raman data corresponding to  $E_L=2.41$  eV is *completely consistent* with that obtained from the Raman data using  $E_L=2.71$  eV. The calculated total intensities for different bias voltages are shown in Fig. 2 as open circles for  $E_L=2.41$  eV and as open stars for  $E_L=2.71$  eV. The trends in the nonmonotonic variation in Raman intensity as a function of the applied cathodic bias are satisfactorily reproduced by the calculations for both the values of  $E_L$ . Figure 2 (inset) shows the variation of  $\gamma(v)$  with the applied voltage.

It is interesting that though the RBM exhibits a non-monotonic variation in the intensity as a function of bias voltage, the TM does not. This can be understood from the fact that the  $\omega_{\text{ph}}$  of the tangential mode does not have a diameter dependence. A small change in  $E_{ii}$  affects the RBM much more than the TM.

We now offer qualitative reasons to understand why  $\gamma_0$  can change under cathodic biasing of the nanotubes. With

negative bias applied to the SWNT, the cations  $\text{Li}^+$  form a space charge double layer around the nanotubes which affect the overlap integral of the  $\pi$  orbitals on adjacent carbon atoms separated by  $a_{\text{cc}}\sim 0.142$  nm. This effect should naively depend on the size of cations. This is indeed the case in our experiments. The effect (seen in Fig. 2) using  $\text{Li}^+$  (ionic size  $\sim 0.12$  nm) is much larger than  $\text{K}^+$  (ionic size  $\sim 0.28$  nm) (data not shown). We believe that large ionic size is also responsible for not seeing the effect under anodic bias (ionic size of ions  $\text{ClO}_4^- \sim 0.8$  nm,  $\text{Cl}^- \sim 0.36$  nm). More theoretical work is needed to quantify this novel effect.

In conclusion, we have shown that the intensity of the radial mode of SWNT varies markedly in a nonmonotonic manner as a function of negative bias. This arises from the reduction of the energy gaps  $E_{ii}$  between the one-dimensional van Hove singularities via a decrease of the overlap integral between the nearest-neighbor carbon atoms. It is tempting to correlate the decrease in  $\gamma_0$  to the observed expansion<sup>4</sup> of the nanotubes along the length under the cathodic bias. This is reasonable because a change in  $\gamma_0$  will alter the electronic contribution to the free energy of the nanotube and hence the equilibrium structural configuration. Further theoretical work could be of value in quantitatively correlating the changes in the electronic structure with the actuator action.

The authors thank Dr. S. Sampath for useful discussions and A. Govindraj for the samples. A. K. S. thanks the Department of Science and Technology for financial assistance.

<sup>1</sup>C. Dekker, Phys. Today **52**, 22 (1999).

<sup>2</sup>C. N. R. Rao, B. C. Satishkumar, A. Govindraj, and M. Nath, Chem. Phys. Chem. **2**, 78 (2001).

<sup>3</sup>M. S. Dresselhaus, G. Dresselhaus, and P. C. Eklund, *Science of Fullerenes and Carbon Nanotubes* (Academic, New York, 1996), Chap. 19.

<sup>4</sup>R. H. Baughman, C. Cui, A. A. Zakhidov, Z. Iqbal, J. N. Barisci, G. M. Spinks, G. G. Wallace, A. Mazzoldi, D. De Rossi, A. G. Rinzler, O. Jasinowski, S. Roth, and M. Kertesz, Science **284**, 1340 (1999).

<sup>5</sup>T. C. Charlier and Ph. Lambin, Phys. Rev. B **57**, R15037 (1998).

<sup>6</sup>P. M. Rafilov, H. Jantoljak, and C. Thomsen, Phys. Rev. B **61**, 16179 (2000).

<sup>7</sup>M. Hulman, W. Plank, and H. Kuzmany, Phys. Rev. B **63**, R081406 (2001).

<sup>8</sup>P. V. Tereadesai, A. K. Sood, D. V. S. Muthu, R. Sen, A. Govindraj, and C. N. R. Rao, Chem. Phys. Lett. **319**, 296 (2000).

<sup>9</sup>A. M. Rao, P. C. Eklund, S. Bandow, A. Thess, and R. E. Smalley, Nature (London) **388**, 257 (1997).

<sup>10</sup>L. Kavan, P. Rapta, and L. Dunsch, Chem. Phys. Lett. **328**, 363 (2000).

<sup>11</sup>A. M. Rao, J. Chen, E. Richter, U. Schlecht, P. C. Eklund, R. C. Haddon, U. D. Venkateswaran, Y.-K. Kwon, and D. Tomnek, Phys. Rev. Lett. **86**, 3895 (2001).

<sup>12</sup>M. A. Pimenta, Phys. Rev. B **58**, R16016 (1998).

<sup>13</sup>M. F. Lin, Phys. Rev. B **62**, 13153 (2000).